

## Article

# Experimental Study of the Influence of Stitched Nylon Threads in Glass-Fiber-Reinforced Polymer Two-Dimensional Multilayer Composite on Tensile Strength

Manuel Alejandro Lira-Martinez <sup>1,\*</sup>, Citlalli Gaona-Tiburcio <sup>2</sup>, Facundo Almeraya-Calderon <sup>2</sup>,  
Jesus Manuel Jaquez-Muñoz <sup>1</sup> and Manuela Alejandra Zalapa-Garibay <sup>1,\*</sup>

<sup>1</sup> Instituto de Ingeniería y Tecnología, Universidad Autónoma de Ciudad Juárez, Av. del Charro No. 450 Nte. Col. Partido Romero, Ciudad Juarez 32310, Chihuahua, Mexico; [jesus.jaquez@uacj.mx](mailto:jesus.jaquez@uacj.mx)

<sup>2</sup> Facultad de Ingeniería Mecánica y Eléctrica (FIME), Centro de Investigación e Innovación en Ingeniería Aeronáutica (CIIA), Aeropuerto Internacional del Norte, Universidad Autónoma de Nuevo León (UANL), Av. Universidad s/n. Cd. Universitaria, San Nicolás de los Garza 66455, Nuevo León, Mexico; [citlalli.gaonatbr@uanl.edu.mx](mailto:citlalli.gaonatbr@uanl.edu.mx) (C.G.-T.); [facundo.almerayacl@uanl.edu.mx](mailto:facundo.almerayacl@uanl.edu.mx) (F.A.-C.)

\* Correspondence: [manuel.lira@uacj.mx](mailto:manuel.lira@uacj.mx) (M.A.L.-M.); [manuela.zalapa@uacj.mx](mailto:manuela.zalapa@uacj.mx) (M.A.Z.-G.)

**Abstract:** Stitched filaments are known to modify the mechanical properties of glass-fiber-reinforced polymers 2D (GFRPs 2D), so studying the effect on mechanical properties is underway to determine the critical variables involved. This research focuses on the study of the tensile strength effect of stitched low-density Barkley FBA BGQS15-15 nylon monofilament on biaxial E-Glass Saertex 830 g/m<sup>2</sup> (+/−45°) cured with Polyester Sypol Resin 8086 CCP using a vacuum infusion process. Four specimens were made with longitudinal distances between the stitched reinforcements of 0.5, 1.0, 1.5, and 2.0 cm, respectively. Tensile strength tests based on standard ASTM D3039 were performed to study how stitching can affect toughness, Young's modulus, deformation, ultimate strength, and yield strength. The results indicated that the stitching increases Young's modulus up to 99.2%, UTS is increased by up to +3.14%, deformation decreases by up to −41.66%, and toughness decreases by up to −36.89%. Although the stitching's main function is to increase interlaminar resistance, it also induces the formation of stress concentrations by the new threads, and premature failure in the matrix was shown.

**Keywords:** composite; delamination; laminated; tensile; interlaminar; fiberglass; polyester



**Citation:** Lira-Martinez, M.A.; Gaona-Tiburcio, C.; Almeraya-Calderon, F.; Jaquez-Muñoz, J.M.; Zalapa-Garibay, M.A. Experimental Study of the Influence of Stitched Nylon Threads in Glass-Fiber-Reinforced Polymer Two-Dimensional Multilayer Composite on Tensile Strength. *Appl. Sci.* **2023**, *13*, 11679. <https://doi.org/10.3390/app132111679>

Academic Editors: Zhongsen Zhang, Ning Liu and Bin Yang

Received: 7 October 2023

Revised: 21 October 2023

Accepted: 23 October 2023

Published: 25 October 2023



**Copyright:** © 2023 by the authors. Licensee MDPI, Basel, Switzerland. This article is an open access article distributed under the terms and conditions of the Creative Commons Attribution (CC BY) license (<https://creativecommons.org/licenses/by/4.0/>).

## 1. Introduction

The aerospace sector is one of the engineering industries where the most importance is given to the innovation of new materials due to the working conditions that aircraft must endure in the distinct phases of flight. The use of composite materials in the aerospace industry has grown since 1980 thanks to their low density, better mechanical properties, and chemical inhibition in comparison to aluminum alloys used, such as 2024, 6061, and 7075 [1,2].

Unfortunately, composite materials have many defects: one of these is delamination, which is a critical failure mechanism in laminate composites caused by high interlaminar stresses coupled with typically exceptionally low through thickness strength. The phenomenon arises because the fibers lying in the plane of a laminate do not provide reinforcement through the thickness, so the composite transfers all external loads into the weaker matrix [3,4].

As far as delamination solution goes, several types of manufacturing that drastically improve interlaminar resistance have been studied, such as 3D weaving, z-pinning, braiding, tufting, and stitching [5–9]. Stitching is one of the most interesting processes since it is much easier to fabricate, and there are also methods used to join different composite

parts [10]. There are several types of stitching, such as tufting and lockstitch, modified lockstitch, chain stitch and one side stitching, to name a few [11–13]. Stitched composites can improve up to 15 times on interlaminar resistance [14]. Chen et al. [15] report that with their stitched method, the fracture toughness can increase 45 times more. Another study made a composite with 0.33 mm diameter steel wires separated by 1.6 mm; this increased interlaminar resistance by 50%, but the manufacturing was non-practical [16]. Another study on carbon fiber/epoxy with Kevlar threads shows that while stitching arrests delamination, there is a variation in tensile strength [17].

Even so, there have been different studies related to issues in formability in stitch composites. Some have shown different methods to fit complex molds by cutting the woven materials and stitching them, which also increases the mechanical properties in the stitch joints [18–24]. Karahan et al. [25] have shown that the density, direction, and pattern of the stitching are critical parameters for optimal mechanical properties. The density of the stitch is particularly important, such as there is a critical stitch density in which a maximum interlaminar resistance is reached. After that, no more resistance gain can be achieved, but a major density stitch can cause a misalignment within the woven material, which then affects its mechanical properties [26]. Karahan et al. [23] in their study showed that stitch density is inversely proportional to tensile strength by the creation of stress concentration in the stitching points. Mulat et al. [27] have shown that stitched composite increases impact resistance, but the damage zone has shown the formation of wrinkles which the unstitched sample does not have, leaving permanent deformation in some samples and a weak recovery after deformation in comparison to the non-stitched sample. To eliminate this, more layers of stitching must be made, but still, deformation recovery is compromised.

The motivation of the present study is to manufacture an unmanned aerial vehicle made of composite material, and since delamination is a concern, the stitching process will be used to increase delamination resistance as it is the process more convenient to us, but more information regarding the effect of the stitching on all the mechanical properties is needed. This investigation is focused on the tensile fracture behavior in four lengths of nylon stitched patterns (0.5, 1.0, 1.5, and 2.0 mm) in a biaxial E-Glass Saertex 830 g/m<sup>2</sup>/Sypon 8086 polyester resin composite. Nylon yarn was chosen because of its low density, tensile and impact strength, and chemically inert property. Flexibility is another beneficial property as it is not as stiff as carbon fiber, Kevlar, or metals, so it does not damage the matrix or reduce flexibility on fiberglass woven when making complex geometries of composite materials [18–24].

## 2. Materials and Methods

The specimens were made via a resin transfer molding (RTM) process with 6 layers of E-Glass Saertex 830 g/m<sup>2</sup> Biaxial (+/−45°) lockstitched with a Brother Exedra sewing machine using an orthogonal weave pattern of 0.3 mm diameter Barkley FBA BGQS15-15 nylon monofilament and polyester resin Composite Envisions 1179 (see Table 1). The specimen's size was made based on ASTM D3039 [28] (250 mm length × 25 mm width × 2.5 mm thickness) with a curing time of 48 h.

**Table 1.** Material properties used for composites.

| Material                      | E-Glass Saertex 830 g/m <sup>2</sup><br>Biaxial (+/−45°) | Barkley FBA BGQS15-15<br>Nylon Monofilament | Polyester Resin<br>Composite Envisions<br>1179 |
|-------------------------------|--|---|--|
| Density, (g/cm <sup>3</sup> ) | 2.76   | 1.6   | 1.089  |
| Filament diameter, μm         | 12   | 300   | --   |
| Modulus of toughness, (GPa)   | 72   | --  | 0.63   |
| UTS, (MPa)                    | 2300–2400  | 1400  | 47   |

Four samples were performed with longitudinal distances between stitches of 0.5, 1, 1.5, and 2 cm, respectively. For this article, the unstitched samples will be named and

labeled as “N” samples, the samples with stitching length distances of 0.5 cm will be simply named “0.5”, the samples with stitching length distances of 1.0 cm will be named as “1.0”, and so on. Five specimens for each sample have been made according to ASTM D3039, identified as consecutive letters. For instance, “N” specimens are labeled as NA, NB, NC, ND, and NE (without stitched); “0.5” specimens are labeled as 0.5A, 0.5B, 0.5C, 0.5D, and 0.5E (stitched with separation of 0.5 cm), and so on (obtaining a total of 25 samples). The stitching separations were made as shown in Figure 1.

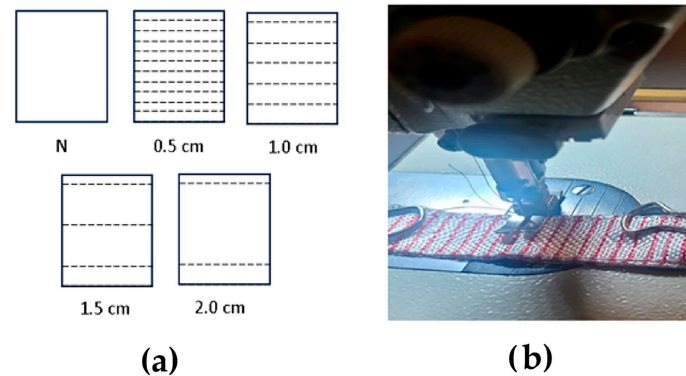


**Figure 1.** Weaving stitch: (a) sample identification patterns; (b) stitch sample on sewing machine.

Tensile tests were made according to the ASTM D3039 standard [28] in a Sintech 20 D universal testing machine. Tensile stress is defined as the ratio of the stretching force applied to the original cross-sectional area of specimen  $A$  [29]:

$$\sigma = F/A, \quad (1)$$

where:

$\sigma$  = tensile stress, MPa (N/ mm<sup>2</sup>);

$F$  = stretching force applied, N;

$A$  = cross-sectional area of the specimen, mm<sup>2</sup>.

When tensile stress is applied, a strain may occur, which is defined as [29]:

$$\epsilon = \frac{l_f - l_0}{l_0}, \quad (2)$$

where:

$\epsilon$  = tensile strain, mm/mm;

$l_f$  = instantaneous length of the specimen, mm;

$l_0$  = initial length of the specimen, mm.

Young’s modulus is the ratio of stress to strain in the elastic region of a stress–strain curve, defined as [29]:

$$E = \frac{\Delta\sigma}{\Delta\epsilon}, \quad (3)$$

where:

$E$  = Young’s modulus, GPa;

$\Delta\sigma$  = change in tensile stress within 2 points of strain, MPa;

$\Delta\epsilon$  = change in tensile strain within 2 points, adimensional.

Toughness is the amount of energy a material can absorb without fracture. Modulus of toughness quantifies the toughness of the material by calculating the total area under the stress–strain curve up until the fracture point of the specimen, defined as [29]:

$$T = \int_{l_0}^{l_f} \sigma dl \quad (4)$$

where:

- $T$  = toughness, MJ/m<sup>3</sup>;
- $l_f$  = instantaneous length of the specimen, mm;
- $l_o$  = initial length of the specimen, mm;
- $\sigma$  = tensile stress, MPa (N/ mm<sup>2</sup>);
- $l$  = length.

### 3. Results

#### 3.1. Tensile Test Results

Figure 2 shows the stress–strain curves obtained from the tensile tests, and Table 2 shows the average tensile test results for each sample as well as percentages of increase/decrease in the stitched samples over the unstitched material. Figure 2a corresponds to the stress–strain diagrams of composite N samples, where there is an average UTS of 187.6337 MPa and a strain of 0.0403 mm/mm. Figure 2b corresponds to the stress–strain diagrams of the 0.5 samples, where an average UTS of 193.5973 MPa and a strain of 0.0235 mm/mm were obtained, in addition to an increase in the slope of the lo curve, which results in a 99.20% higher average Young’s modulus compared to the N sample. Figure 2c corresponds to the 1.0 samples, where an average UTS of 189.7865 MPa was obtained, an average deformation of 0.0272 mm/mm, and a slight decrease in the slope, which indicates that Young’s modulus decreases in comparison with the 0.5 sample. Figure 2d corresponds to the stress–strain diagrams of the 1.5 samples, where an average UTS of approximately 188.9748 was obtained, an average strain of 0.0307 mm/mm, and a slight decrease in the slope concerning the previous sample, which indicates that Young’s modulus decreases. Finally, Figure 2e corresponds to the stress–strain diagrams of the 2.0 samples, where an average UTS of 188.6894 MPa and an average strain of 0.0334 mm/mm were obtained, resulting in a decrease in the slope of twice the curve, indicating a decrease in Young’s modulus from the previous curves.

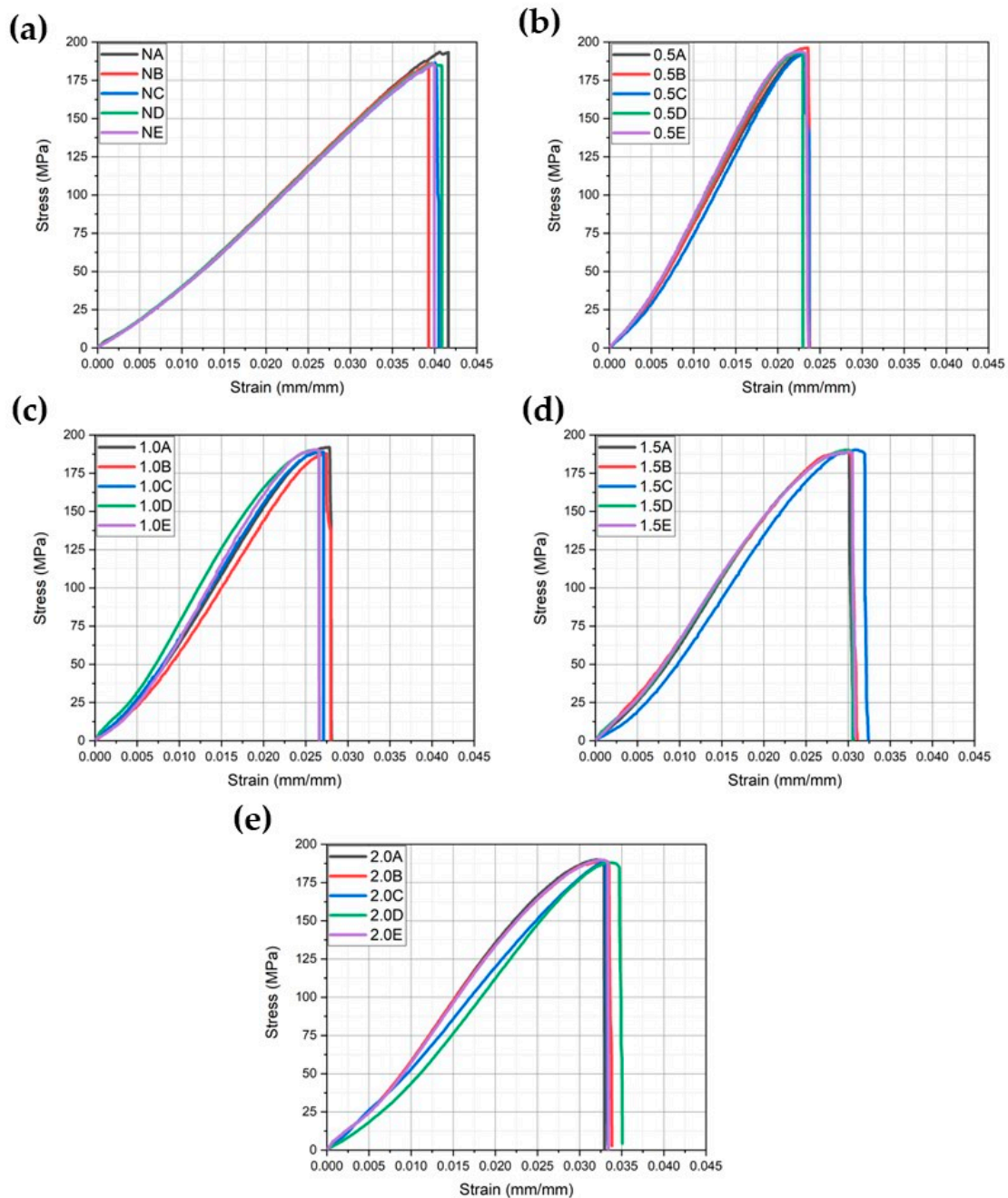
**Table 2.** Mechanical properties obtained from tensile test.

| Sample | UTS (MPa)         | Strain (mm/mm)   | E (GPa)           | T (MJ/m <sup>3</sup> ) |
|--------|-------------------|------------------|-------------------|------------------------|
| N      | 187.6337          | 0.0403           | 5.1137            | 3.7400                 |
| 0.5    | 193.5973 (+3.17%) | 0.0235 (−41.66%) | 10.1870 (+99.20%) | 2.3599 (−36.89%)       |
| 1.0    | 189.7865 (+1.14%) | 0.0272 (−32.47%) | 8.6891 (+69.91%)  | 2.7196 (−27.28%)       |
| 1.5    | 188.9748 (+0.71%) | 0.0307 (−23.85%) | 7.7145 (+50.85%)  | 3.192486 (−14.64%)     |
| 2.0    | 188.6894 (+0.56%) | 0.0334 (−16.99%) | 6.7200 (+31.41%)  | 3.407956 (−8.87%)      |

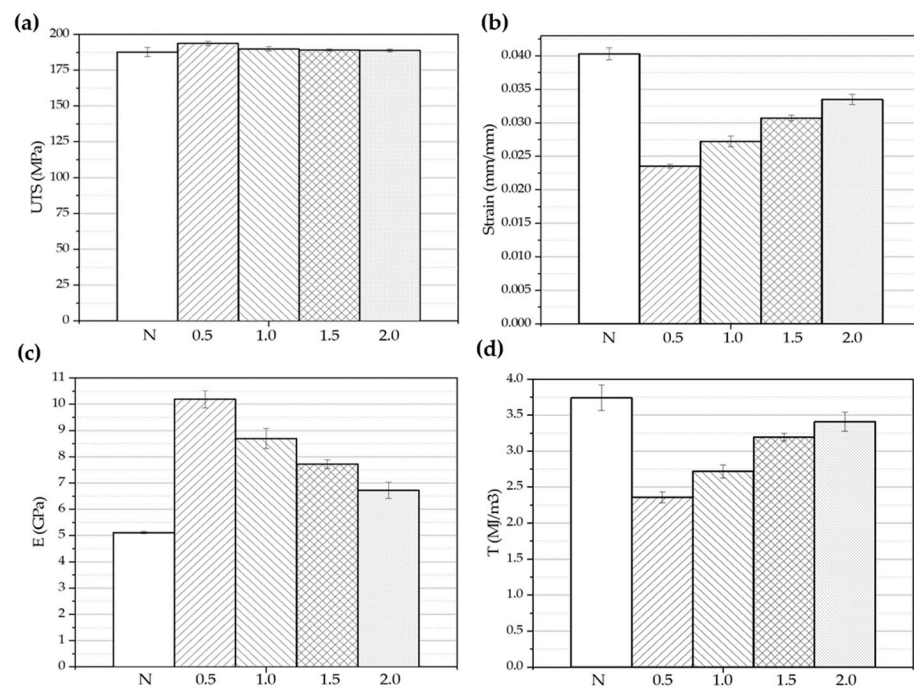
We can deduce that as the length between the stitching increases, Young’s modulus decreases the same way as the UTS. Studies have mentioned that the more stitching separation there is, the less tensile resistance there is, yet these studies used a rigid thread [23,25], so flexibility in the thread is another major parameter to be considered. In the case of deformation, as the length separation of the stitching increases, the deformation increases slightly; this behavior can be attributed to the fact that the stitching threads carry most of the energy and reduce the stress within the matrix, and more energy is required to propagate the crack through the matrix, increasing tensile resistance, while at the same time the stitching reduces the propagation of delamination, which is a common mechanism on composite that also reduces tensile resistance [29–37].

Figure 3 shows the average mechanical properties comparison of the different samples obtained from the stress–strain diagrams. Table 3 shows the standard deviation of all the mechanical properties, in which all values are 5% less than the average, meaning the values tend to be close to the mean, and thus it is statistically reliable. Figure 3a shows the comparison of the average UTS of all samples. An increase of 3.17% was obtained in the 0.5 samples over the unstitched samples, but a decrease is shown between 1.0, 1.5, and 2.0 samples. Even so, there is a 0.56% increase in the 2.0 sample over N sample, which is the sample with most minor UTS of them all. This variation within the stitched

samples is attributed to the loose region between the stitching points, which affected resin permeability, resulting in the creation of voids and porosity [38]. Figure 3 also shows that the standard deviation in N sample is 3.2; even though this is a very good value, it is still higher than the stitching samples values of 1.49, 1.5, 0.81, and 1.01, respectively, which indicates that by adding the stitching, the properties are more stable. It has been reported that stitching reduces tensile strength because of the creation of stress concentrations at the stitch point, misalignment, crimping, and even breakage on fibers [30,39–41]. But it has also been reported that stitching increases tensile strength [42,43].



**Figure 2.** Stress–strain curves from tensile tests. (a) N specimens, (b) 0.5 specimens, (c) 1.0 specimens, (d) 1.5 specimens, and (e) 2.0 specimens.



**Figure 3.** Mechanical properties comparison of the different samples obtained from the stress–strain diagrams, (a) UTS, (b) Young’s modulus, (c) strain, and (d) toughness.

**Table 3.** Standard deviation on mechanical properties obtained from tensile test.

| Sample | UTS (MPa)    | Strain (mm/mm) | E (GPa)      | T (MJ/m <sup>3</sup> ) |
|--------|--------------|----------------|--------------|------------------------|
| N      | 3.20 (1.70%) | 0.0009 (2.27%) | 0.04 (0.87%) | 0.17 (4.72%)           |
| 0.5    | 1.49 (0.77)  | 0.0003 (1.31%) | 0.32 (3.18%) | 0.07 (3.20%)           |
| 1.0    | 1.50 (0.79%) | 0.0007 (2.80%) | 0.38 (4.38%) | 0.09 (3.34%)           |
| 1.5    | 0.81 (0.43%) | 0.0004 (1.43%) | 0.16 (2.18%) | 0.05 (1.69%)           |
| 2.0    | 1.01 (0.54%) | 0.0007 (2.28%) | 0.30 (4.56%) | 0.13 (3.86%)           |

Figure 3b shows the average Young’s modulus in all samples, in which 0.5 samples have increases of 99% over the N sample, and as the length separation of the stitching increases, Young’s modulus also decreases, making the 2.0 sample the lower value in comparison to all the other stitched samples, but there is still an increase of 31.41% over the N sample. It can be deduced that the smaller the length distance within the stitching, the more rigid the composite becomes. We can attribute this to the flexibility of nylon.

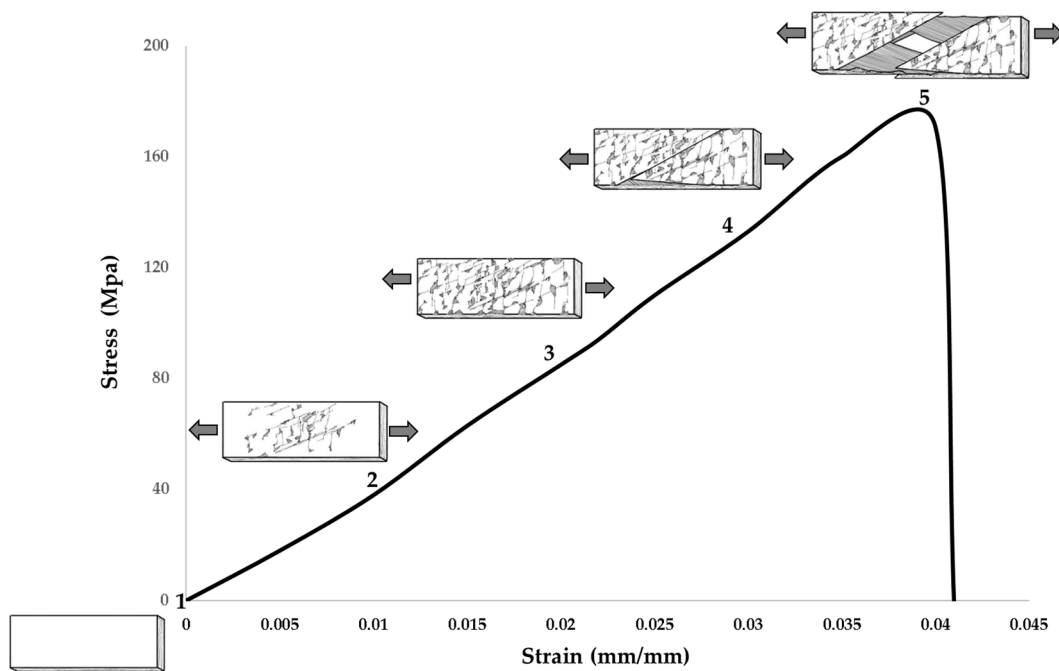
In Figure 3c, a comparison of the average deformation on all samples is shown; the N samples present the maximum value, 0.5 samples decrease the deformation by 41.66%, 1.0 samples decrease by 32.47%, 1.5 samples decrease by 23.85%, and 2.0 samples reduce their deformation by 16.99%. Therefore, the length distance of the stitching is inversely proportional to the deformation of the samples.

Figure 3d shows the toughness results, where it is observed that the N sample has the maximum value. The 0.5 samples have the minimum value, decreasing by 36.89% over the N sample; by this, we can deduce that as the stitching length separation increases, toughness increases. From what can be shown, stitched strength slightly increases tensile strength and decreases toughness because they help stabilize the weave structure of the fibers within the composite.

### 3.2. Fracture Analysis

Figure 4 shows sketches of the evolution of the fracture in the N samples during the tensile test. The fracture mechanism is divided into five stages, starting from the zero point of the

graph. Stage 1 corresponds to the starting point, where zero stress equals zero deformation; separation phenomena between the stitching and the matrix occur as the tensile stress increases. At stage 2, due to the stresses generated in the center of the sample, pre-cracking on the matrix begins to appear, and there is little matrix detachment, making internal pull-out fibers occur. The pre-cracking has trajectories like the direction of the fibers within the composite. In stage 3, small fractures in the matrix within the direction of the fibers appear, and transversal cracks are formed, which contribute to the detachment of a greater amount of matrix from the composite, resulting in internal fiber pull-out. During stage 4, the fibers externally pull out due to bigger fractures and cracks, and matrix detachment begins. This is a chain reaction that ends at stage 5 by separating the sample into two parts, and the crack line coincides with the direction of the reinforcing fibers.



**Figure 4.** Evolution of the N sample fracture mechanism.

Figure 5 shows the SEM images of the fracture analysis of the N sample, where stages 3, 4, and 5 were identified as shown in Figure 4. Figure 5a shows a fractured NA specimen, where we can observe the beginning of the fibers pulling out from the matrix on the surface of the fracture, in addition to the areas that correspond to where each of the stages of the fracture are located. This is because the fracture of a composite material is progressive, starting from the center of the specimen and moving to its end. Figure 5b,c correspond to stage 3 of the fracture, where cracks are observed in the direction of the stitching and vertical cracks that favor the detachment of the matrix. Figure 5d,e correspond to zone 4 of the fracture, where the detachment of the matrix and pull-out of the fibers are observed, indicating the material's weakening. Figure 5f,g correspond to the fracture, where the fibers are observed to be separated from the matrix, resulting in delamination [30].

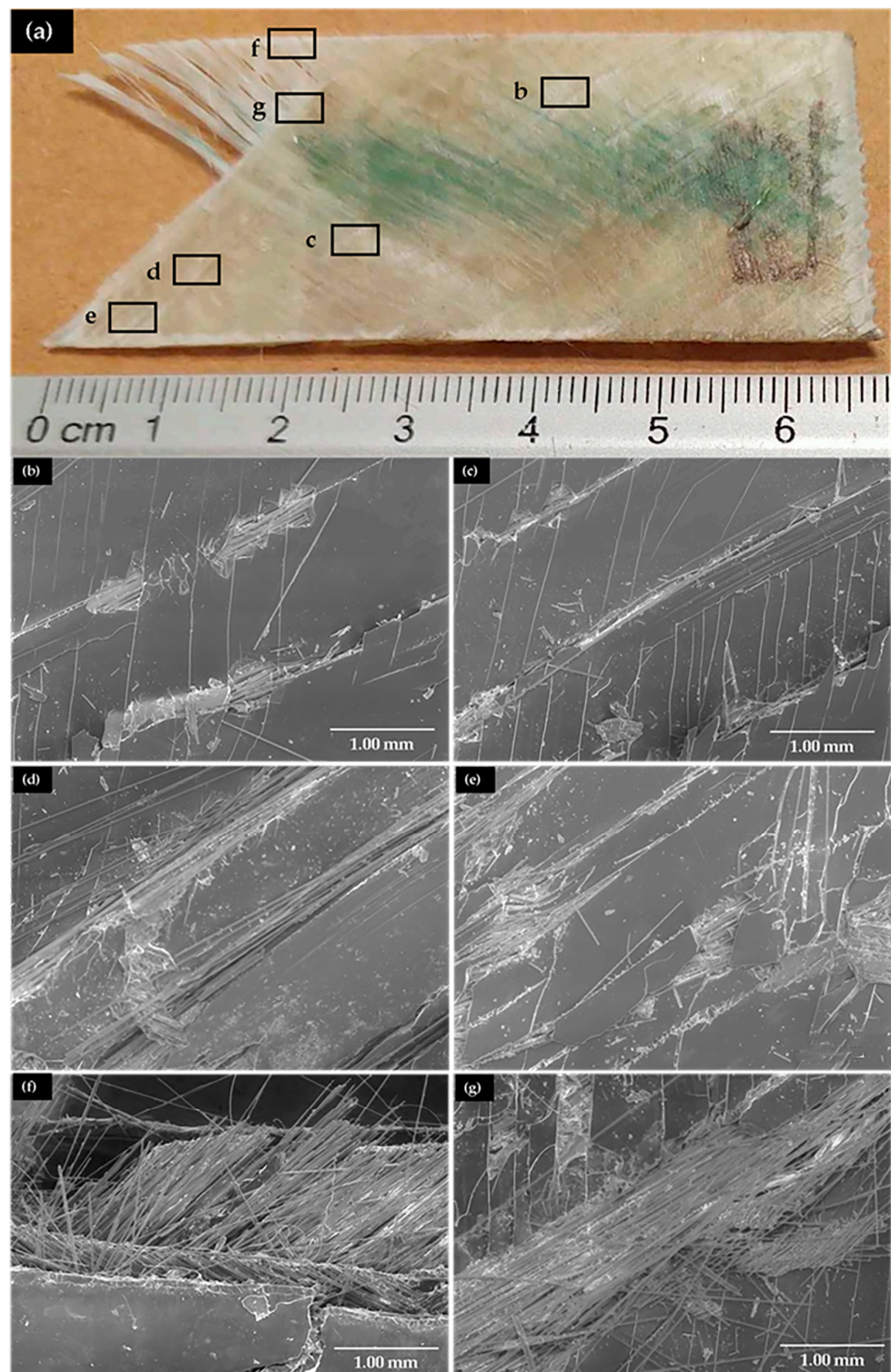


**Figure 5.** (a) Tensile fractured NA specimen, (b,c) stage 3 of fracture, the pre cracking on matrix, (d,e) stage 4, formation of transverse cracks, (f,g) stage 5, fracture, pull-out of fibers, and detachment of matrix.

The fracture mechanisms in the stitched samples were almost identical, with no significant difference between each other to report. By avoiding redundancy, the 0.5C sample was chosen as a representative specimen on the stitched samples to make the consecutive analysis. Figure 6 represents sketches of the evolution of the fracture in the stitched samples. The fracture analysis is also divided into five stages. Stage 1 commences



the tensile test, where zero stress equals zero strain, and separation between the stitching, the fibers, and the matrix occurs as tensile stress increases. In stage 2, the matrix begins to crack as the tensile stress increases. As shown in Figure 3b, the strain can decrease by as much as 50% because the stitching helps to keep the fiberglass in place. The stitching points behave as stress concentrators and thus prevent cracks from propagating along the fiberglass of the reinforcements, thus delaying fiberglass pull-out. In stage 3, the cracks significantly begin to grow transverse to the samples, and small fractures start to appear within the matrix as well as the N sample. Internal pull-out fibers start and are shown as whitening zones on the surface.

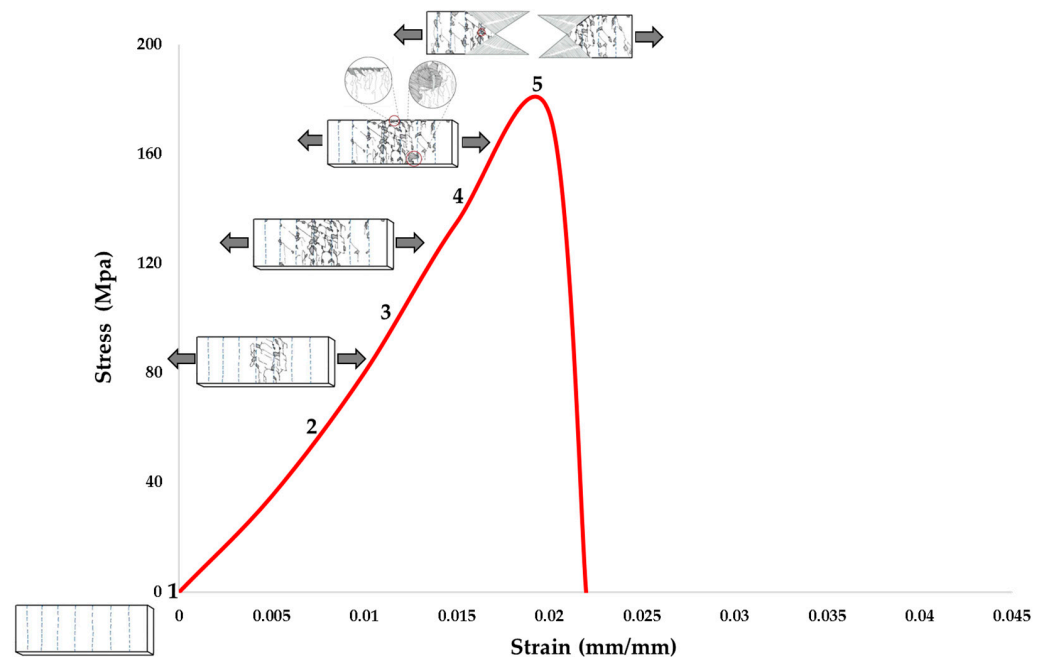


**Figure 6.** Evolution of the stitched sample fracture mechanism.

In stage 4, cracking increases in the areas surrounding the stitching and in the transverse direction of the sample, as well as the detachment of the matrix; this can be observed in stage 4 of Figure 6. At this stage, the external pull-out phenomenon begins in the stitching, which is considered to be a chain reaction. In stage 5, the fracture of the stitched samples is represented, where it is observed that in the fracture, there is greater detachment of the matrix due to the concentration of stresses in the stitching.

Figure 7 shows the SEM images of the fracture analysis of a stitched sample, where stages 3, 4, and 5 are identified, which are explained in Figure 6. Figure 7a shows a fractured stitched sample. Figure 7b,c correspond to stage 3 of the fracture, where cracks are observed in the direction of the stitching and vertical cracks that favor the detachment of the matrix. In addition, the effect of the stitching is observed, which is reflected in the stress concentration in the matrix and affects its detachment. Tigh regions made by the stitching propagate micro-crackings on the matrix [38]. Figure 7d,e correspond to zone 4 of the fracture, where the detachment of the matrix, tearing of the fibers, and exposure of the superficial fibers are observed to a greater extent, unlike the N samples. In this case, it is observed that despite the greater detachment of the matrix, the fibers remain intertwined due to the stitching arresting them. Figure 7f,g correspond to the fracture where the fibers are completely exposed and stitching is fractured as well; however, the fibers remain intertwined. Unlike the N sample, the pull-out phenomenon is retained because the stitching keeps the fibers in place. The stitched sample fractures include additional sewing thread pull-out from composite and/or sewing thread breakage during loading, which is

caused by the interaction of the third directional fibers with the delamination. Therefore, the crack dissipates more energy during the propagation process [44].

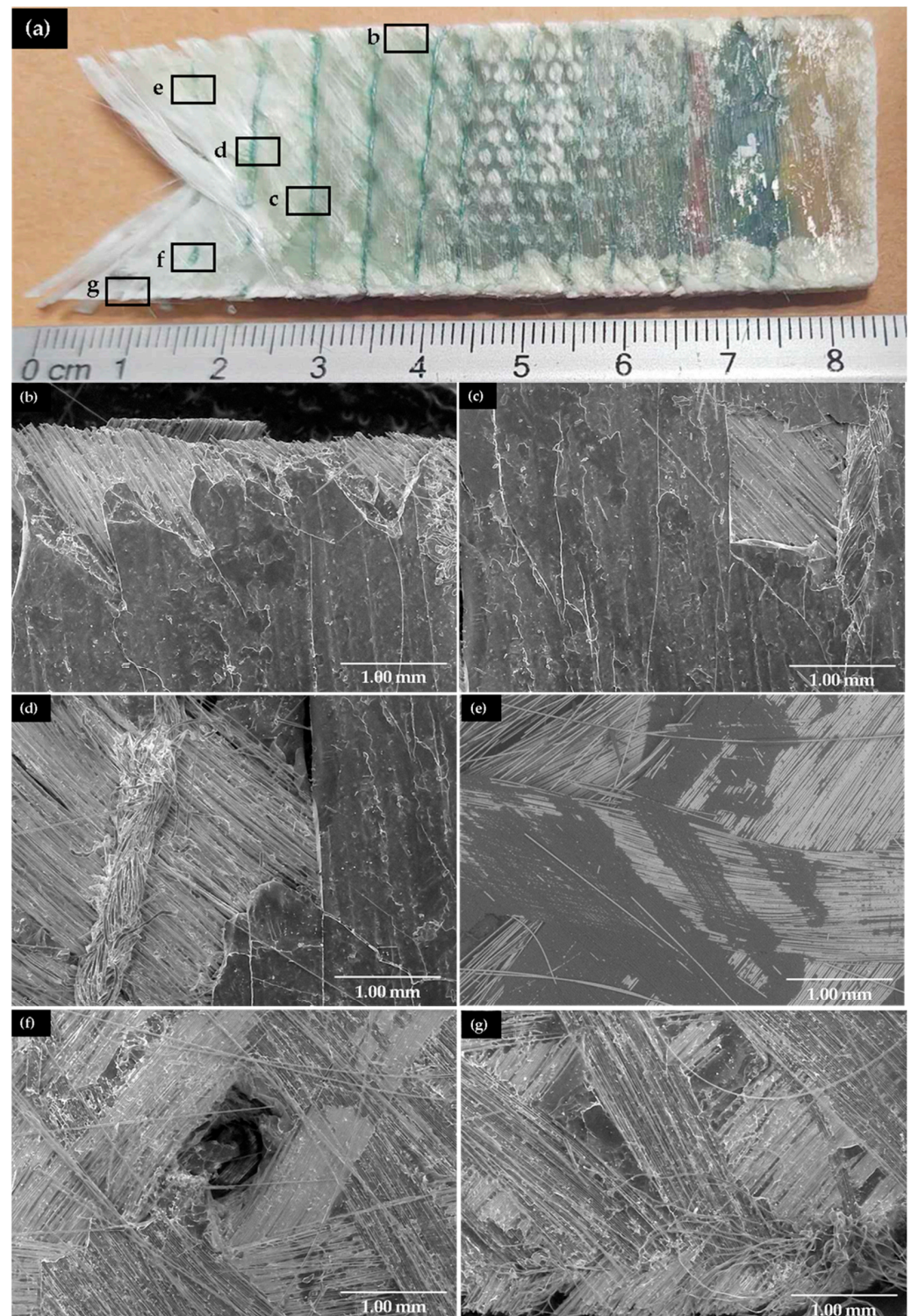


**Figure 7.** (a) Tensile fracture in the stitched sample, (b,c) stage 3 of fracture, the pre-cracking on matrix and beginning of detachment of matrix, (d,e) stage 4, formation of transverse cracks, (f,g) stage 5, fracture, pull-out of fibers and detachment of matrix.

As seen in Figures 5 and 7, the stitching helps hold the glass fibers in place, which helps increase Young's modulus (Figure 3b) as the stitching length separation is shorter.

However, strain and toughness (Figure 3b,d) decrease because the stitching does not allow the glass fibers to move even if the matrix fractures. The UTS is not modified, considering that fiberglass has the greatest properties involved in the composite material. It can be deduced that it is for this reason.

#### 4. Discussion

Tensile test and fracture analysis on fiberglass/polyester composites stitched with 0.3 mm nylon thread have been studied. One sample unstitched and four different samples were used, with longitudinal distances between the stitches of 0.5, 1.0, 1.5, and 2.0 cm, for which the tensile test results showed that the stitched samples have, over the unstitch material, slight increases of 3.17%, 1.14%, 0.71%, and 0.56% on UTS. This increase is attributed to the stitching threads that help to carry more energy, but the decrease in tensile strength as the longitudinal distance between stitches is longer is attributed to the fact that it has less thread to absorb energy, and that loosens regions between the stitch's points, which affects resin permeability. The strain of the stitched samples has reductions of 41.66%, 32.47%, 23.85%, and 16.99% over the unstitched samples because of the stitching points, which also contributes to the increases in Young's Modulus of 99.20%, 69.91%, 50.85%, and 31.41% over the unstitched samples, but decreases in toughness of 36.89%, 27.28%, 14.64%, and 8.87%.

Fracture analysis shows that although the stitching generates a stress concentration in the matrix and promotes its detachment as the tension increases, it also keeps the glass fibers in place. In Table 4, fracture stages are summarized as follows: In stage 1, tensile starts and no visual indication is shown. In stage 2, both samples start to show minor matrix cracks. Stitched samples cracks are retained and concentrated within the stitched points. Unstitched samples have more strain than stitched samples, and cracks disperse all over the surface. In stage 3, cracks increase, and small zones start to fracture in the matrix. Internal pull-out is shown on both samples, but in stitched samples it is presented near the stitching zone, while in the unstitched sample it is presented all over the surface. In stage 4, external pull-out fibers are shown because of major cracks and fractures within the matrix and the stitching, and again in the stitched samples, the cracks, fracture, and fibers are retained by the now remaining stitching points, while in the unstitches samples the damage is spread all over the specimens and fibers are pulling out from the composite.

**Table 4.** Comparison of fracture stages between unstitched and stitched samples.

| Stage | Unstitched Sample  | Stitched Sample  |
|-------|--|--|
| 1     | Tensile test starts.   | Tensile test starts.   |
| 2     | Separation between the stitching, fibers, and the matrix starts to occur as tensile stress increases. Minor matrix cracks start to appear. | Separation between the stitching, fibers, and the matrix starts to occur as tensile stress increases. Minor matrix cracks start to appear, retained by stitched points.                  |
| 3     | Cracks increase significantly and small fractures start to appear in the matrix; internal pull-out fibers start.                           | Matrix cracks increase significantly, and small fractures start to appear near the stitching points; internal pull-out fibers start.   |
| 4     | Major matrix cracks and fractures are growing; external pull-out fibers have appeared.   | Major matrix cracks and fractures are showed near the stitching points; external pull-out fibers have appeared, retained by stitching points. Some stitches are being fractured as well. |
| 5     | Fracture of the composite.   | Fracture of the composite.   |

With these results, it has been shown that the shorter the stitching length distance is, the more displacement is obtained on the tensile test, which is directly proportional to the material toughness, but tensile resistance is compromised. A harder resin is recommended for stitching composites.

Stitched composite materials are complex materials to analyze since there are so many variables that can drastically change the properties of the materials. While the stitched materials results show an increase in tensile properties over the unstitched ones, new stress concentrators

as stitching points weaken the matrix, which is a concern for how the material will hold up on multiple forces applications, such as unmanned aerial vehicles. A possible solution could be to use a harder resin, such as epoxy. More studies on different mechanical tests with the same patterns as presented must be conducted on whether to use the material or not.

## 5. Conclusions

In this investigation, the tensile fracture behavior in four lengths of nylon stitched patterns (0.5, 1.0, 1.5, and 2.0 mm) on a glass fiber/polyester resin composite in comparison to the normal unstitched composite has been analyzed. The stitched process was used to prevent delamination, but the effect of the stitched composite itself on the mechanical properties was unknown. Nylon yarn was chosen due to the flexibility in the fiber, but the damage of the stitched composite within the matrix was a concern.

The elasticity of the nylon stitches contributes to almost double Young's modulus in comparison to the unstitched sample by keeping the glass fibers in place within the composite, but deformation, toughness, and matrix integrity were compromised. All of these were proportional to the length distance between the stitching points. Also, a slight increase in tensile test was achieved.

Because of that, fracture analysis shows that stitching helps to retain the energy and the distribution of cracks within the stitching points, as opposed to the unstitched material, in which cracks were distributed all over the material length. This impacts the matrix as it shows major damage near the stitching zone in comparison with the unstitched material.

This material is meant to be used for an unmanned aerial vehicle, so more mechanical testing needs to be conducted, and a change to a harder resin is recommended for stitched composites.

**Author Contributions:** Conceptualization, M.A.L.-M., C.G.-T., F.A.-C. and M.A.Z.-G.; data curation, M.A.L.-M., C.G.-T. and M.A.Z.-G.; formal analysis, M.A.L.-M., F.A.-C. and J.M.J.-M.; investigation, M.A.L.-M.; methodology, M.A.Z.-G.; visualization, M.A.L.-M.; writing—original draft, M.A.L.-M. and M.A.Z.-G.; writing—review and editing, C.G.-T., J.M.J.-M. and M.A.Z.-G. All authors have read and agreed to the published version of the manuscript.

**Funding:** This research was funded by the Mexican National Council for Science and Technology (CONACYT) and the Universidad Autonoma de Ciudad Juarez (UACJ).

**Institutional Review Board Statement:** Not applicable.

**Informed Consent Statement:** Not applicable.

**Data Availability Statement:** The data presented in this study are available on request from the corresponding author.

**Acknowledgments:** The authors acknowledge The Academic Body UACJ CA-100 "Ingenieria Aplicada y Tecnologia de Materiales" and UANL—CA-316 "Deterioration and integrity of composite materials".

**Conflicts of Interest:** The authors declare no conflict of interest.

## References

1. Mouritz, A. *Introduction to Aerospace Materials*, 1st ed.; Woodhead Publishing: Cambridge, UK, 2012; pp. 306–336.
2. Abramovich, H. *Stability and Vibrations of Thin-Walled Composite Structures*, 1st ed.; Woodhead Publishing: Cambridge, UK, 2017; pp. 1–18.
3. Brigante, D. *New Composite Materials: Selection, Design and Application*, 1st ed.; Springer: Napoli, Italy, 2014; pp. 35–44.
4. Wisnom, M. The Role of Delamination in Failure of Fibre-Reinforced Composites. *Philos. Trans. R. Soc. A* **2012**, *370*, 1850–1870. [[CrossRef](#)] [[PubMed](#)]
5. Composites World. Available online: <https://www.compositesworld.com/articles/3-d-preformed-composites-the-leap-into-leap> (accessed on 10 August 2023).
6. Saleh, M.N.; Soutis, C. Recent advancements in mechanical characterisation of 3D woven composites. *Mech. Adv. Mater. Mod. Process.* **2017**, *3*, 12. [[CrossRef](#)]
7. Gu, H.; Zhili, Z. Tensile behavior of 3D woven composites by using different fabric structures. *Mater. Des.* **2002**, *23*, 671–674. [[CrossRef](#)]

8. Pankow, M.; Justusson, B.; Riosbaas, M.; Waas, A.; Yen, C. Effect of fiber architecture on tensile fracture of 3D woven textile composites. *Compos. Struct.* **2019**, *225*, 111139. [[CrossRef](#)]
9. Dahale, M.; Neale, G.; Lupicini, R.; Cascone, L.; McGarrigle, C.; Kelly, J.; Archer, E.; Harkin-Jones, E.; McIlhagger, A. Effect of weave parameters on the mechanical properties of 3D woven glass composites. *Compos. Struct.* **2019**, *223*, 110947. [[CrossRef](#)]
10. Glaessgen, E.; Ivatury, S.; Clarence, C. *Modeling the Influence of Stitching on Delamination Growth in Stitched Warp-Knit Composite Lap Joints*; NASA Technical Reports Server (NTRS): Washington, DC, USA, 1999; pp. 1–10.
11. Sassi, S.; Tarfaoui, M.; Ben Yahia, H. An investigation of in-plane dynamic behavior of adhesively-bonded composite joints under dynamic compression at high strain rate. *Compos. Struct.* **2018**, *191*, 168–179. [[CrossRef](#)]
12. Byun, J.-H.; Song, S.-W.; Lee, C.-H.; Um, M.-K.; Hwang, B.-S. Impact properties of laminated composites with stitching fibers. *Compos. Struct.* **2006**, *76*, 21–27. [[CrossRef](#)]
13. Mozafary, V.; Payvandy, P.; Bidoki, S.-M.; Bagherzadeh, R. Predicting the influence of seam design on formability and strength of nonwoven structures using artificial neural network. *Fibers Polym.* **2013**, *14*, 1535–1540. [[CrossRef](#)]
14. Reeder, J. *An Evaluation of Mixed-Mode Delamination Failure Criteria*; NASA Technical Reports Server (NTRS): Washington, DC, USA, 1992; pp. 1–54.
15. Chen, L.; Ifju, P.G.; Sankar, B.V. A Novel Double Cantilever Beam Test for Stitched Composite Laminates. *J. Compos. Mater.* **2001**, *35*, 1137–1149. [[CrossRef](#)]
16. Tarfaoui, M.; Hamitouche, L.; Khammassi, S.; Shah, O. Examination of the Delamination of a Stitched Laminated Composite with Experimental and Numerical Analysis Using Mode I Interlaminar. *Arab. J. Sci. Eng.* **2020**, *45*, 5873–5882. [[CrossRef](#)]
17. Karahan, M.; Ulcay, Y.; Eren, R.; Karahan, N.; Kaynak, G. Investigation into the Tensile Properties of Stitched and Unstitched Woven Aramid/Vinyl Ester Composites. *Text. Res. J.* **2009**, *80*, 880–891. [[CrossRef](#)]
18. Zhong, T.; Hu, H. Formability of weft-knitted fabrics on a hemisphere. *Autex Res. J.* **2007**, *7*, 245–251.
19. Bekampiene, P.; Domskiene, J. Experimental analysis of the influence of stress concentrators on the buckling of woven materials under uniaxial tension. *Int. J. Mater. Form.* **2010**, *3*, 211–214. [[CrossRef](#)]
20. Molnár, P.; Ogale, A.; Lahr, R.; Mitschang, P. Influence of drapability by using stitching technology to reduce fabric deformation and shear during thermoforming. *Compos. Sci. Technol.* **2007**, *67*, 3386–3393. [[CrossRef](#)]
21. Abtew, M.A.; Boussu, F.; Bruniaux, P.; Loghin, C.; Cristian, I.; Chen, Y.; Wang, L. Forming characteristics and surface damages of stitched multi-layered para-aramid fabrics with various stitching parameters for soft body armour design. *Compos. Part A Appl. Sci. Manuf.* **2018**, *109*, 517–537. [[CrossRef](#)]
22. Allaoui, S.; Boisse, P.; Chatel, S.; Hamila, N.; Hivet, G.; Soulat, D.; Vidal-Salle, E. Experimental and numerical analyses of textile reinforcement forming of a tetrahedral shape. *Compos. Part A Appl. Sci. Manuf.* **2011**, *42*, 612–622. [[CrossRef](#)]
23. Karahan, M.; Ulcay, Y.; Karahan, N.; Kuş, A. Influence of Stitching Parameters on Tensile Strength of Aramid/Vinyl Ester Composites. *Mater. Sci.* **2013**, *19*, 67–72. [[CrossRef](#)]
24. Dransfield, K.; Baillie, C.; Mai, Y.-W. Improving the delamination resistance of CFRP by stitching—A review. *Compos. Sci. Technol.* **1994**, *50*, 305–317. [[CrossRef](#)]
25. Tan, K.; Yoshimura, A.; Watanabe, N.; Iwahori, Y.; Ishikawa, T. Further investigation of Delamination Reduction Trend for stitched composites. *Compos. Sci. Technol.* **2015**, *118*, 141–153. [[CrossRef](#)]
26. Liu, D. Delamination Resistance in Stitched and Unstitched Composite Plates Subjected to Impact Loading. *J. Reinf. Plast. Compos.* **1990**, *9*, 59–69. [[CrossRef](#)]
27. Huang, T.; Jiao, G.; Zhao, L. Fatigue Behavior of Stitched Carbon/Bismaleimide Composite Laminates. *J. Reinf. Plast. Compos.* **2007**, *26*, 297–303. [[CrossRef](#)]
28. *ASTM D3039*; Standard Test Method for Tensile Properties of Polymer Matrix Composite Materials. 4th ed. ASTM International: West Conshohocken, PA, USA, 2001; pp. 1–19.
29. Martin, W. *Materials for Engineering*, 3rd ed.; Woodhead Publishing: Cambridge, UK, 2006; pp. 185–214.
30. Zhao, N.; Rödel, H.; Herzberg, C.; Gao, S.-L.; Krzywinski, S. Stitched glass/PP composite. Part I: Tensile and impact properties. *Compos. Part A Appl. Sci. Manuf.* **2009**, *40*, 635–643. [[CrossRef](#)]
31. Bibo, G.A.; Hogg, P.J. The role of reinforcement architecture on impact damage mechanisms and post-impact compression behaviour. *J. Mater. Sci.* **1996**, *31*, 1115–1137. [[CrossRef](#)]
32. Hosur, M.V.; Adya, M.; Alexander, J.; Jeelani, S.; Vaidya, U.; Mayer, A. Studies on Impact Damage Resistance of Affordable Stitched Woven Carbon/Epoxy Composite Laminates. *J. Reinf. Plast. Compos.* **2003**, *22*, 927–952. [[CrossRef](#)]
33. Ou, Y.; González, C.; Vilatela, J.J. Understanding interlaminar toughening of unidirectional CFRP laminates with carbon nanotube veils. *Compos. Part B Eng.* **2020**, *201*, 108372. [[CrossRef](#)]
34. Kuwata, M.; Hogg, P. Interlaminar toughness of interleaved CFRP using non-woven veils: Part 1. Mode-I testing. *Compos. Part A Appl. Sci. Manuf.* **2011**, *42*, 1551–1559. [[CrossRef](#)]
35. Hamer, S.; Leibovich, H.; Green, A.; Intrater, R.; Avrahami, R.; Zussman, E.; Siegmann, A.; Sherman, D. Mode I interlaminar fracture toughness of Nylon 66 nanofibrillated interleaved carbon/epoxy laminates. *Polym. Compos.* **2011**, *32*, 1781–1789. [[CrossRef](#)]
36. Yasaee, M.; Bond, I.; Trask, R.; Greenhalgh, E. Mode I interfacial toughening through discontinuous interleaves for damage suppression and control. *Compos. Part A Appl. Sci. Manuf.* **2012**, *43*, 198–207. [[CrossRef](#)]
37. Zheng, N.; Huang, Y.; Liu, H.-Y.; Gao, J.; Mai, Y.-W. Improvement of interlaminar fracture toughness in carbon fiber/epoxy composites with carbon nanotubes/polysulfone interleaves. *Compos. Sci. Technol.* **2017**, *140*, 8–15. [[CrossRef](#)]

38. Yaakob, M.Y.; Husin, M.A.; Abdullah, A.; Mohamed, K.A.; Khim, A.S.; Fang, M.L.C.; Sihombing, H. Effect of Stitching Patterns on Tensile Strength of Kenaf Woven Fabric Composites. *Int. J. Integr. Eng.* **2019**, *11*, 70–79. [[CrossRef](#)]
39. Larsson, F. Damage tolerance of a stitched carbon/epoxy laminate. *Compos. Part A Appl. Sci. Manuf.* **1997**, *28*, 923–934. [[CrossRef](#)]
40. Takatoya, T.; Susuki, I. In-plane and Out-of-plane Characteristics of Three-dimensional Textile Composites. *J. Compos. Mater.* **2005**, *39*, 543–556. [[CrossRef](#)]
41. Reeder, J.R. Stitching vs. a Toughened Matrix: Compression Strength Effects. *J. Compos. Mater.* **1995**, *29*, 2464–2487. [[CrossRef](#)]
42. Kang, T.; Lee, S. Effect of stitching on the mechanical and impact properties of woven laminate composite. *J. Compos. Mater.* **1994**, *28*, 1574–1587. [[CrossRef](#)]
43. Mouritz, A.P. Fracture and tensile fatigue properties of stitched fibreglass composites. *Proc. Inst. Mech. Eng. Part L J. Mater. Des. Appl.* **2004**, *218*, 87–93. [[CrossRef](#)]
44. Jang, B.; Shih, W.; Chung, W. Mechanical Properties of Multidirectional Fiber Composites. *J. Reinf. Plast. Compos.* **1989**, *8*, 538–564. [[CrossRef](#)]

**Disclaimer/Publisher’s Note:** The statements, opinions and data contained in all publications are solely those of the individual author(s) and contributor(s) and not of MDPI and/or the editor(s). MDPI and/or the editor(s) disclaim responsibility for any injury to people or property resulting from any ideas, methods, instructions or products referred to in the content.